Spatially extended populations reproducing logistic map

Witold Dzwinel

[1] AGH Institute of Computer Science, Al. Mickiewicza 30, 30-059 Krakow, Poland
dzwinel@agh.edu.pl

Abstract

Spatial distribution of individuals and the way they interact with their neighbors and environment are important factors, which are neglected in simplistic ecological models. Therefore, the logistic equation (LE) fails in describing evolution of majority of real populations. More intriguing is the inverse problem. What conditions must spatially extended systems (SES) satisfy to reproduce the logistic map? To address this dilemma we define 2-D coupled map lattice with local rule mimicking the logistic formula. We show that for growth rates $k \leq k_\infty$ (k_∞ is the accumulation point) the global evolution of the system reproduces exactly the cascade of period doubling bifurcations. However, for $k > k_\infty$, instead of chaotic modes, the cascade of period halving bifurcations are observed. Consequently, the microscopic states at the lattice nodes resynchronize producing dynamically changing spatial patterns. By downscaling of the system and assuming intense mobility of individuals over the lattice, the correlations can be destroyed and the local rule remains the only factor deciding about the evolution of the whole colony. We found the class of "atomistic" rules for which uncorrelated spatially extended population matches the logistic map both for pre-chaotic and chaotic modes. We concluded that the global logistic behavior can be expected for a colony with high mobility of individuals whose local behavior is governed by semi-logistic rule with long dispersal and competition radiuses. The populations forming dynamically changing spatial clusters and stable patterns behave in a different way than the logistic model and reproduce at least steady-state fragment of the logistic map.

Keywords: logistic map, spatially extended systems, cellular automata, patterns, chaos

1 Introduction

Most of fundamental ecological factors, such as individual behavior, population diversity, species abundance, and population dynamics, exhibit spatial variation. This trivial property has many important consequences on the evolution of organisms and populations. On the one hand, the evolution can produce spatially stable colonies of individuals enabling the optimal use of the environmental resources. On the other, spatial dynamics of individuals allows for better exchange of genetic material thus increases the fitness factor of the entire colony. To understand the role of spatial variations in evolution, many ecological models were studied.

The simplest are the coupled logistic maps (CLM) which do not include space in an explicit way. The CLM model consists of only two patches coupled by dispersal, with dynamics in each patch governed by the logistic map. As shown in [1,2,3] the coupling can stabilize individually chaotic populations or make a periodic population more chaotic. However, CLM have serious limitations. The maps can be used for studying subdivided distant populations. Meanwhile, to investigate the tightly coupled colonies involving the interactions over the entire living area, explicit space is required [4], as it is, e.g., in the reaction-diffusion approaches [5-9]. In these continuous models the dynamics of population density is dictated by partial differential equations (PDE). As show in [9], the motion of simple organisms can produce stable and regular strips and checkerboard like patterns that can be formed by diffusion driven instabilities. Moreover, the movement of multiple species can change the outcome of competition and predation in the predator-pray problem [9].

For simulating the evolution of discrete entities, over discrete or continuous time and space, many epidemic models employ simple rules instead of PDEs. For example, in the cellular automata (CA) models the individuals are located in the nodes of 2-D (or 1-D) lattice and evolve in discrete time [8, 10-14]. According to microscopic CA rule, the offspring are dispersed across a *dispersal neighborhood* and individuals have a death rate depending on the population density in a *competition neighborhood*. The results obtained from CA approaches can be refined by using continuous individual-based model (IBM) [15] in which discrete objects evolve in continuous time and space, and moment closure models involving mean-field approximations [16,17]. The clustering of individuals and influence of the dispersal and competition on global dynamics of the whole population is scrutinized by using, so called, spatial logistic equation (SLE) [4]. SLE differs from the logistic equation only in that the term x^2 (x is a population density and $x \in [0,1]$) of the logistic equation is replaced with an integral expression. In [4] the authors concluded that the populations can grow much slower or much faster than would be expected from the non-spatial logistic model. Eventually, different steady-states are gained. Moreover, they can reached their maximum growth rate at densities $x \neq 1/2$, i.e., unlike it comes out from the logistic formula. These types of behavior can be controlled both by values of dispersal/competition radiuses and their ratio.

This SLE approach focuses only on the steady-state dynamics and its analytical approximations. The conditions of convergence of the known spatially extended models to the 0-D logistic-model for the full span of dynamic modes, including bifurcation cascades and chaotic modes were not addressed yet. Therefore, the important questions arise. Do the spatially extended populations, which reproduce the full evolution scenario from the logistic map, exist? If they do, what conditions must be satisfied? The positive answer on the first question is of a fundamental importance. Otherwise, the logistic law could not be treated as "the law" anymore, because every population is attributed by the space it occupies.

To answer this problem we use the cellular automata (CA) model. Cellular Automata paradigm allows for modeling of relatively large, spatially extended systems (SES), and is general enough to represent variety of types of systems and evolution scenarios. In the first section we define the continuum 2-D coupled map lattice and we show that logistic equation is not a scale-free model for SES. We downscale continuum CA system by consecutive discretization of the

states of automata up to binary representation. Consequently, we refine this binary model to simulate the population of individuals evolving on the CA lattice. Then we derive the microscopic CA rules, which allow the entire population for reproducing the dynamics of the logistic model. We explore the properties of this system by studying various factors which control dynamics of the entire population such as: the mobility of individuals, number of neighbors, dispersal and competition radiuses. We discuss the role of emerging patterns in control of population dynamics. Finally, we summarize the conclusions.

2 Coupled map lattice

We consider a spatial single-specie logistic model, which dynamics is governed by the logistic map:

$$x^{n+1} \rightarrow k \cdot x^n \left(1 - x^n\right) \tag{1}$$

where $x \in [0,1]$ represents the current population density while n is the generation number and k is the growth rate. The time evolution of this map is well understood (e.g. [23]). If the value of k is between 0 and 1, the equilibrium at $x=0$ is stable. If $1<k<3$, $x = f(k) = \left(1 - \dfrac{1}{k}\right)$ is the fixed point of iteration. At $k=3$ there is a period-doubling bifurcation, starting a period-doubling cascade that leads to the onset of chaos at $k>k_\infty=3.569945672\ldots$, where k_∞ is the accumulation point [18]. For $k>4$ the map generates negative numbers.

As shown in [2,4] the logistic equation often fails to describe the evolution of realistic populations. The reasons are manifold, e.g.:

1. heterogeneity of the environment,
2. dispersal may not increase linearly with density or there may be a time delay in the operation of dispersal and/or competition,
3. time delays can occur in structured populations when density affects vital power at particular sizes or ages,
4. the random collision of individuals assumed in the logistic equation, often referred to as the "mean-field" assumption, may not represent interactions among organisms well.

As shown, e.g., in [2,5-7,14,19-21], deviations from logistic behavior for spatially extended systems (SES) are often manifested by production of patterns. These spatial patterns can be treated not only as a pure consequence of population dynamics, i.e., the effect of energy minimization in dissipative open system, but as a built-in self-control mechanism for stable evolution.

To understand better the factors making the simple logistic model different from realistic evolution of populations, we try to find spatially extended systems which global behavior follows exactly the logistic law. Particularly, they should produce the same *path-to-chaos* scenario. Then we could specify the conditions of such the systems existence. Cellular automata (CA) paradigm is a very efficient and flexible model of SES [10,12]. It represents a synthetic model of universe in which physical laws are expressed in terms of local rules **R**. As shown schematically in Fig.1, our problem reduces then to derive such the CA microscopic rules **R** for which the entire system mimics the logistic model. Finding such the rules in mathematically rigorous way is a very hard inverse problem, so we try to guess the solution basing on some hypotheses and observations.

At first, we check if the logistic model is scale-free, i.e., if it can be used as the local rule over various spatial (and spatio-temporal) resolutions. If it does, we will have the first solution instantly. If not, we can try to construct a better rule on the basis of this first approximation.
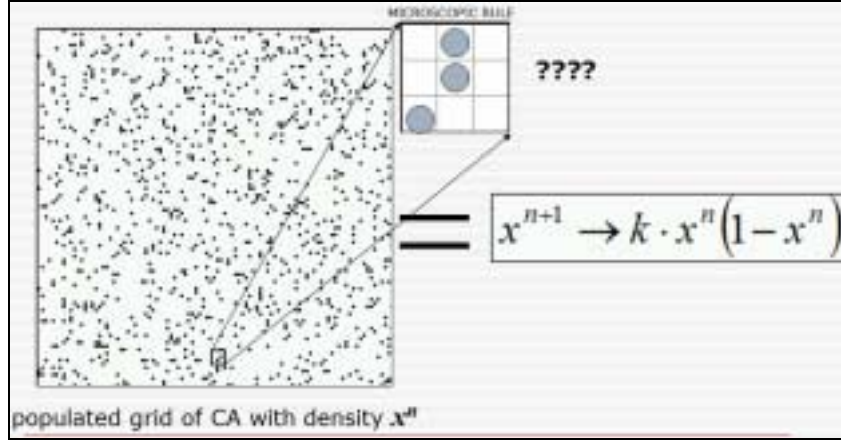
Fig.1 We are looking for a CA microscopic rule, which produces global logistic map.

Let us consider continuous state cellular automata. We define a two-dimensional squared lattice of nodes $\Im(l,m)=[\{l,m\},\ l=1,...,M;\ m=1,...,M]$. One-dimensional CA does not simplify the problem too much and it imposes additional unrealistic constrains on population evolution. The lattice is periodic, homogeneous and bounded but large enough the edge effects to be neglected. We assume that $M=100\text{-}300$ because, as we observe, for the most of simulations the structures with correlation lengths <100 produce adequate statistics. The values X_{kl} in the nodes representing their states are the real numbers from $[0,1]$ interval. Every $\{l,m\}$ node interacts only within its closest neighborhood $\Omega(l,m)$. The neighborhood of $\{l,m\}$ node is the sum of *dispersal* D and *competition* C neighborhoods $\Omega(l,m)=\Omega_D(l,m,R)\cup\Omega_C(l,m,r)$. We assume for generality that $\Omega_D(l,m,R)$ and $\Omega_C(l,m,r)$ can be different, where R and r are *dispersal* and *competition* radiuses, respectively. For example, the Moore neighborhood has only $N=8$ adjacent nodes and $r=R=1$. The *dispersal* reflects "biological power" of the population, which is proportional to the population size, i.e., $\Omega_D(l,m,R)\rightarrow kY_D$, while the *competition* is the selection pressure caused by the shrinking resources (space) due to population growth, i.e., $\Omega_C(l,m,r)\rightarrow(1\text{-}Y_C)$, where Y_D and Y_C are the local population densities in R and r radiuses, respectively.

Initially, the X^0_{lm} values are generated by random number generator $rnd_{lm}\in[0,1]$. The population evolves in space and time. The CA system is updated synchronously according to the set of rules **R**:

$$X_{lm}^{n+1} \rightarrow \mathbf{R}\Big[X_{lm}^{n}, \Omega_D(l,m,R), \Omega_C(l,m,r)\Big], \tag{2}$$

where X_{lm}^{n} denotes the state of $\{l,m\}$ node in nth generation (time). Because R and r can be different and $X_{lm}^{n}\in[0,1]$, we assume that if $X_{lm}^{n+1}>1$ in Eq.2 then X_{lm}^{n+1} is rounded to 1.

Let us assume, that the automata in the system are independent, i.e., $r=R=0$ and the rule **R** is defined as follows:

$$\mathbf{R}: X_{lm}^{n+1} = k \cdot X_{lm}^{n} \cdot \Big(1 - X_{lm}^{n}\Big). \tag{3}$$

Such the system is locally logistic in every node of CA lattice. As shown in [22], for $k=4$ the subsequent X_{lm} values in each node match well the following statistical distribution:

$$X_{lm} = \frac{1}{2} \cdot (1 - \cos(\pi \cdot rnd_{lm})),$$ (4)

where $rnd_{kl} \in (0,1)$ are random numbers generated by a uniform random number generator. The expectation value over the entire lattice $x = E(X) = 1/2$ and the variance $\sigma^2 = 1/8$. The system is globally stable and asymptotic for $1 < k < 4$ and $\lim_{n \to \infty} x^n \to x^*$. However, if we start all the automata from exactly the same initial value, we obtain the logistic map shown in Figs.2:a1,a2.
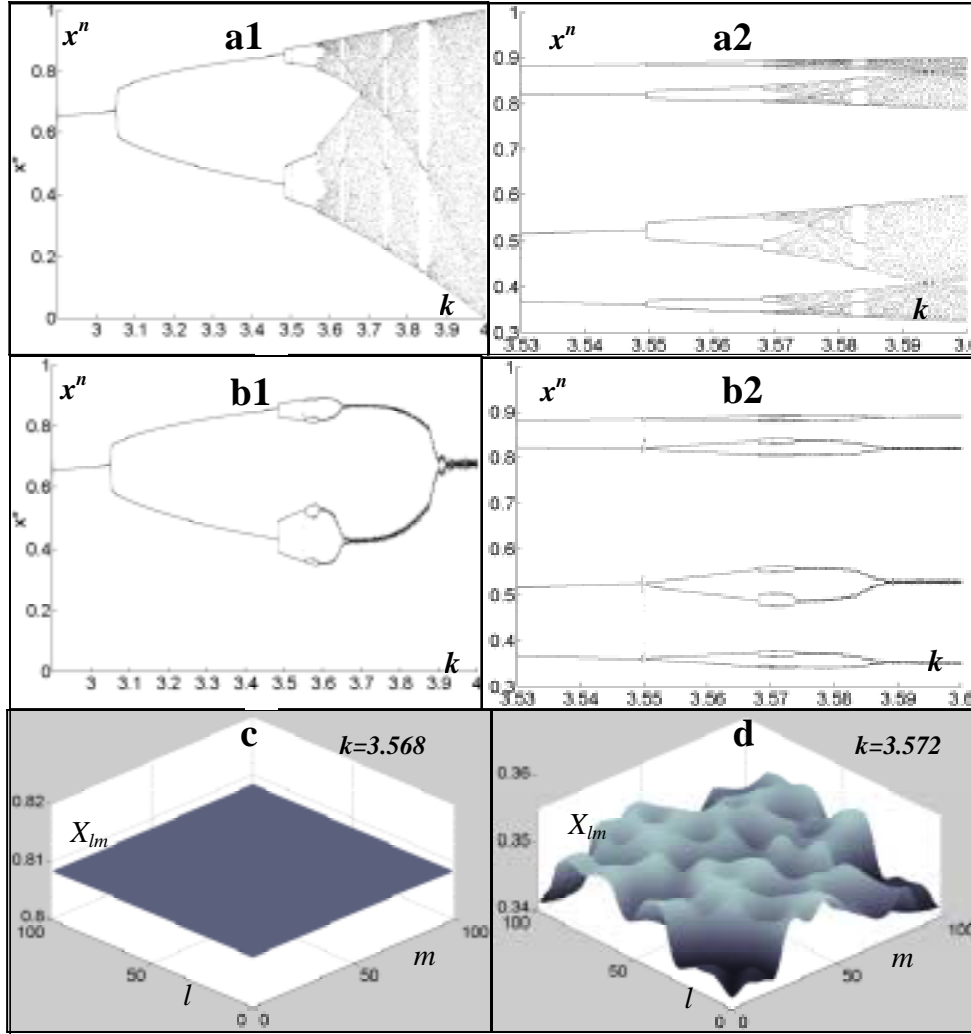
Fig.2 Figure (a1) and its zoomed part (a2) show the classical logistic map. The maps from figures (b1) and (b2) were obtained for 2-D coupled map lattice defined by Eq.5. Figures (c) and (d) shows the snapshots ($n = 2500$) of the surfaces representing CA states on the 100x100 lattice close to the accumulation point k_∞. Some imperfections in logistic maps (e.g., the lack of initial phase of bifurcations) are caused by approximations used during their generation.

Let us define the lattice of CA coupled by the logistic local rule **R** which involves interactions between neighboring cells:

$$\mathbf{R}: X_{lm}^{n+1} = k \cdot Y_{lm}^n \cdot (1 - Y_{lm}^n), \quad Y_{lm} = \frac{1}{(N+1)} \sum_{i \in \Omega(l,m) \cup \{l,m\}} X_i,$$ (5)

where $r=R$, $N = (2r+1)^2 - 1$ is the number of neighboring nodes, Y_{kl} is the local average of CA states over $\Omega(l,m)$. By averaging Eq.(5) over entire lattice we obtain that:

$$x^{n+1} = k \cdot x^n \cdot (1 - x^n) - k \cdot \sigma_n^{\,2} \qquad (6)$$

where:

$$\sigma_n^{\,2} = E\left[(Y_{lm}^n)^2\right] - E^2(Y_{lm}^n), \quad x^n = \sum_{lm} X_{lm}^n / M^2$$

The first part of Eq.6 is responsible for global dynamics of the whole system while the second one represents spatial, local modes. As follows from Eq.6, the coupled CA system can mimic exactly the logistic model provided that no spatial patterns are created during the system dynamics (i.e., $\sigma_n^2 = 0$). Because $0 < x^n < 1$, the interval of possible x^n values becomes narrower with increasing variance.

   The results from simulation displayed in Figs.2:b1,b2 show that for $k < k_\infty$ the entire system reproduces exactly the logistic *path-to-chaos* scenario represented by the cascade of period doubling bifurcations. For $k < k_\infty$, the CA system converges fast to uniform and synchronized lattice of automata (see Fig.2c) with zero variance ($\sigma_n^2 = 0$, in Eq.6). As shown in [23], for a class of coupled logistic lattices the temporal and spatial periods of the observed patterns undergo successive period doubling bifurcations with decreasing coupling strength. Eventually, for $k > k_\infty$ the value of Lyapunov exponent becomes greater than 0, and propagating round off error destroys the coupling. Then, instead of chaotic modes observed in Figs.2:a1,a2, the entire system produces the cascade of period halving bifurcations (compare Figs.2 a1,a2 to b1,b2). Finally, for $k > 3.9$, the value of x stabilizes and fluctuates around the fixed point ($x^* \approx 2/3$). As shown in Fig.3a, the variance σ_n^2 increases with k for $k > k_\infty$. The non-zero variance signals the appearance of spatial patterns (see Fig.2d). Simultaneously - similarly to the CA nodes in decoupled lattice of automata defined by Eq.3 - individual CA lattice nodes become chaotic (see Fig.3b). This way, the fully synchronized and globally periodic system undergo resynchronization in $k = k_\infty$ and eventually - for larger k - becomes globally static (fluctuating) and locally chaotic.
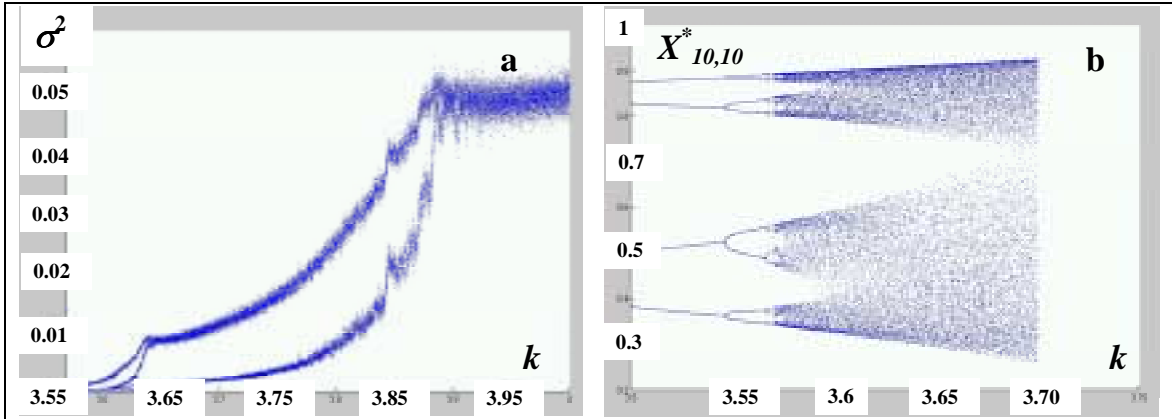
Fig.3 a) The variance σ^2 and (b) the map of the values of $X_{10,10}^n$ (see Eq.5) in $\{10,10\}$ node from Eq.6 with increasing k.

The lattice of continuum state CA can be treated as a system of interacting environments (CA nodes) with identical population capacities and infinite number of states **s**. The value of X_{lm} represents then the population density in the *{l,m}* environment (CA node) while the value of **s** defines the maximum number of individuals which can populate a single CA node (environment). Discretization and consequent decreasing the number of states can be interpreted as downscaling

of the system. The neighborhood $\Omega(l,m)$ is shrinking simultaneously with decreasing population capacity of the environments.
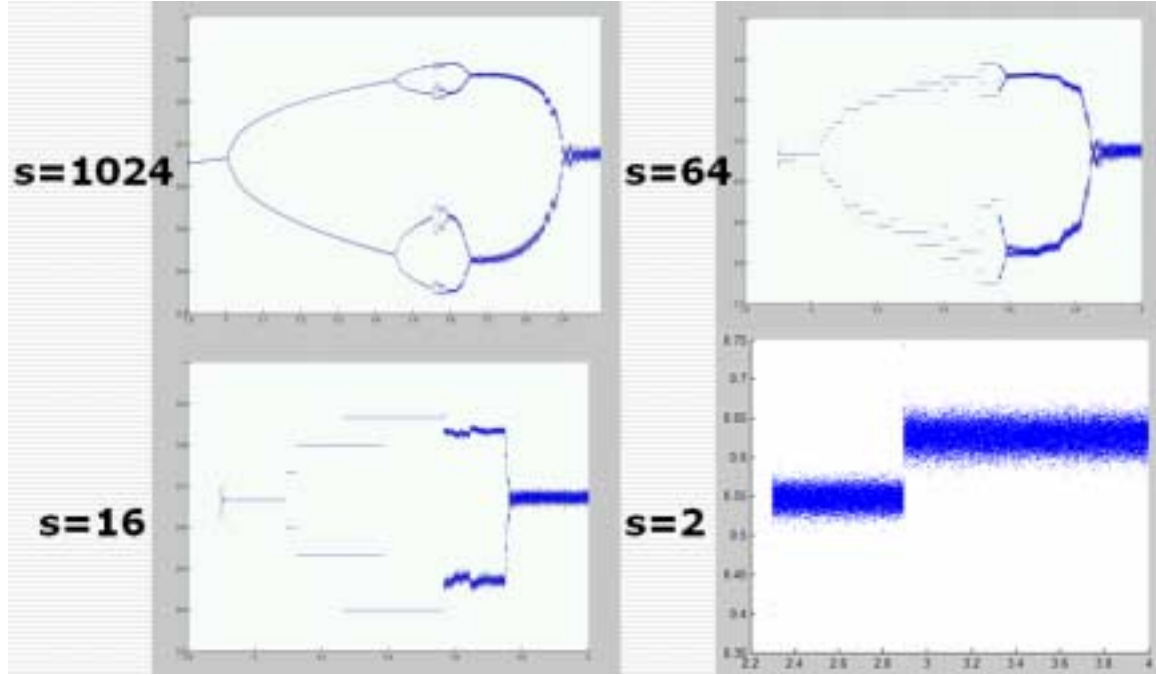
Fig.4 The maps for CA lattices with increasing discretization of CA states. The value of **s** stands for the number of possible CA states.

As shown in Fig.4, the number of bifurcations decreases due to discretization of the CA states. Eventually, for **s**=2 we obtain binary CA with discretized logistic rule **R** (Eq.5):

$$\mathbf{R}: a = k \cdot Y_{lm}^{n} \cdot \left(1 - Y_{lm}^{n}\right), \quad X_{lm}^{n+1} = \begin{cases} 1 & \text{if } a > \dfrac{1}{2} \\ 0 & \text{if } a < \dfrac{1}{2} \end{cases}, \quad Y_{lm} = \frac{1}{9} \sum_{i \in \Omega(l,m) \cup \{l,m\}} X_i, \quad X \in \{0,1\}. \tag{7}$$

As displayed in Fig.4 (**s**=2), the global dynamics of this system is very different from the logistic map. For $k<2.3$ the average population density $x=0$ while for $k>2.3$ it fluctuates chaotically around some stable attractors.

Summarizing, we have demonstrated that the logistic equation is not a truly scale free model when applied for the lattice of continuum state cellular automata. We have showed that only for $k<k_\infty$, the CA system exactly reproduces the cascade of period doubling bifurcations. The appearance of chaotic modes for $k>k_\infty$, destroys synchronization and tamed global chaotic behavior. Instead of global chaos, the spatial patterns emerge. Downscaling (discretization) of the CA system destroys also the pre-chaotic cascade of period doubling bifurcation. However, in contrast to multiple-state CA, the binary cellular automata system manifests clear chaotic behavior displayed in Fig.4 (**s**=2).

On the basis of these hints, we can expect that the candidate of SES, which can reproduce the logistic map, should be searched among binary CA systems with local rules enabling to eliminate correlations responsible for creation of spatial patterns.

3   Binary Cellular Automata

The binary CA periodic lattice can be interpreted as the living space for individuals. When an individual occupy the node $\{l,m\}$ then $X_{lm}=1$, otherwise $X_{lm}=0$. For the Moore neighborhood

($r=R=1$) every *{l,m}* node "sees" only its $N_N=8$ adjacent nodes. Initially, the lattice is populated randomly and the average population density $x=x^0$. The population evolves in space and time.

Unlike in the previous section, we consider now a binary CA system, which dynamics is governed by two repetitive rules:

- **R1:** random walk within a given time period ΔT, realized using lattice gas automata (e.g. [6])
- **R2**: evaluation round:

$$\varepsilon_{lm}^{n\Delta T+1} \rightarrow \mathbf{R2}\Big[X_{lm}^{nT}, \Omega_D(l,m,R), \Omega_C(l,m,r)\Big]$$

$$X_{lm}^{n\Delta T+1} = \begin{cases} 1 \text{ if } rnd < \varepsilon_{lm}^{n+1} \\ 0 \text{ if } rnd > \varepsilon_{lm}^{n+1} \end{cases} \qquad [8]$$

where: X_{lm} – the binary CA states, Ω_D and Ω_C - the dispersal and competition neighborhood, respectively, ε_{lm} – the probability that $X_{lm}=1$ in the following generation, *rnd* – random number, $rnd \in (0,1)$.

The random walk represents the randomization factor which breaks local correlations. The value of ΔT is equal to the number of walking steps and defines the extent of randomization. We can assume that for adequately large value of $\Delta T=\Delta T_{MAX}$ the CA population becomes fully uncorrelated. Such the "uncorrelated" system can be simulated by using much simpler model than random walk. The random collisions and motion of individuals during ΔT_{MAX} can be mimicked by their random scatter of over the CA lattice after each evaluation round **R2**. It means that the time-step between subsequent **R2** rounds is equal to ΔT_{MAX}.

We define the stochastic rule **R2** as a set of probabilities $a_{1/0\,i}$:

$$\mathbf{R2} = \Big\{ 0 \le a_{1,i} \le 1 \wedge 0 \le a_{0,i} \le 1; X_{lm}^{n+1} = 1 \Big\} \qquad (9)$$

that in *n+1* timestep, X_{lm} with *i* nonzero neighbors in $\Omega(l,m)$ remains/becomes populated.

This type of rule represents a broad class of 2-D cellular automata, including totalistic CAs, as well as, many well known specific automata [10] such as the "game of life", parity rule automata, Vichniac annealing rule, spin glasses, and many others. As shown in Fig.1, we are looking for a local rule **R2**, for which the 2-D CA system will mimic, as a whole, the logistic formula from Eq.(1).

To find proper **R2** rules, we assume that before employing the rule **R2** synchronously in all lattice nodes the distribution of individuals is random. This is due to application of **R1** rule for $\Delta T=\Delta T_{MAX}$ according to the current population density x^n. As shown in [24], for randomly scattered points on the plane, the number of individuals in a circle of radius r will follow a Poisson distribution. Therefore, it is justified that the statistical distribution of the number of populated CA nodes in the neighborhood $\Omega(l,m)$ for each *{l,m}* node can be approximated by binomial distribution. Then the population density *x* evolves in time according to the following formula:

$$x^{n+1} \rightarrow px^n \sum_{i=0}^{N_C} a_{1i} \binom{N_C}{i} (x^n)^i (1-x^n)^{N_C-i} + q(1-x^n) \sum_{i=0}^{N_D} a_{0(N_D-i)} \binom{N_D}{i} (x^n)^{N_D-i} (1-x^n)^i \qquad (10)$$

where $$x^n = \sum_{l,m}^{M} X_{lm}^n / M^2$$

and $0<p<1$ and $0<q<1$ are "environmental" probabilities of survival of existing individuals and newborns, respectively. We are looking for such the rules **R2** which reduce the Eq.10 to Eq.1. Comparing Eq.1 with Eq.10, after some algebra we obtain finally that:

$$p \cdot \left(\frac{N_C \cdot a_{1i}}{N_C - i} \right) + q \cdot \left(\frac{N_D \cdot a_{0i+1}}{i+1} \right) = k; \ a_{1N_C} = a_{00} = 0 \tag{11}$$

$$\text{for} \quad i = 1,...,\max(N_C, N_D) - 1$$

where k is the biotic potential from Eq.1. The maximum value of k, k_{max}, for which Eq.10 can be reduced to Eq.1, is computed from (11) assuming that $N_C=N_D=N_N$, $a_{0i}=a_{1i}=1$ and $i=N_N/2$. We obtain that:

$$k_{max} = 4 \cdot \left(\frac{N_N \left(\frac{p+q}{2} \right) + p}{N_N + 2} \right) \quad \wedge \quad \lim_{N_N \to \infty} (k_{max}) = 4 \cdot \left(\frac{p+q}{2} \right). \tag{12}$$

As it comes out from Eqs.12, the "uncorrelated" population can reproduce the whole logistic map in macro-scale for certain microscopic rules **R** deduced from Eq.11 in case of infinite neighborhood $N_N \to \infty$. For the Moore neighborhood $(N_N=8)$, the system reproduces only the part of it, i.e., the fragment for $k \leq k_{max}=3.6$. The number of rules satisfying Eq.11 is infinite. A few exemplar rules are collected in Table.1. Except of the set 3 in Table 1, the remaining sets mimic approximately dispersal and competition rules from the logistic equation. Despite that these microscopic rules are not perfect copies of the resulting macroscopic behavior they are of a very similar nature.

Table 1. A few examples of CA microscopic stochastic rules computed from Eq.11 and producing chaotic behavior for "uncorrelated" CA populations $(N_N=8, p=q=1)$. The CA systems governed by these rules replicate the logistic equation with $k<=k_{max}=3.6$.

No.	1		2		3		4	
neigh. i	a_{1i}	a_{0i}	a_{1i}	a_{0i}	a_{1i}	a_{0i}	a_{1i}	a_{0i}
0	0	0	0.4	0	1	0	0	0
1	0	0.45	0.7	0.4	1	0.325	0	0.45
2	0.9	0.9	0.9	0.7	1	0.614	0.7	0.386
3	1	0.9	1	0.9	1	0.85	1	1
4	1	1	1	1	1	1	1	1
5	0.9	1	0.9	1	1	1	1	1
6	0.9	0.9	0.7	0.9	0.9	0.7	0.9	0.7
7	0.45	0	0.4	0.7	0.45	0	0.45	0
8	0	0	0	0.4	0	0	0	0

Let us reduce the number of possible solutions of Eq.11 focusing on the totalistic cellular automata. Then the subsequent state of each $\{l,m\}$ node depends on the probability $a_i \in (0,1)$

computed for all individuals in $\Omega(l,m)$ neighborhood including the $i=\{l,m\}$ node. By substituting $a_i=a_{1i}=a_{0i+1}$ $(a_{-1}=a_{00}=1)$ and for $p=q=1$ the Eq.11 reduces to a unique solution:

$$a_i = k \cdot \frac{(i+1)}{(N_N+1)} \cdot \left(1 - \frac{i}{N_N}\right) = k \cdot Y_i\left(1 - \widetilde{Y}_i\right) \wedge k \in (0, k_{max}] \qquad (13)$$

where $1<k\leq k_{max}$. The values of Y and $\widetilde{Y}_i$ are the maximum local population density and the population density in the closest neighborhood of $\{l,m\}$ node, respectively. The values of resulting probabilities are shown in Table 1 as the second set (2) of exemplar rules. It is worth to mention that the Eq.13 is very similar - but not identical - to microscopic logistic equation defined by Eq.7.
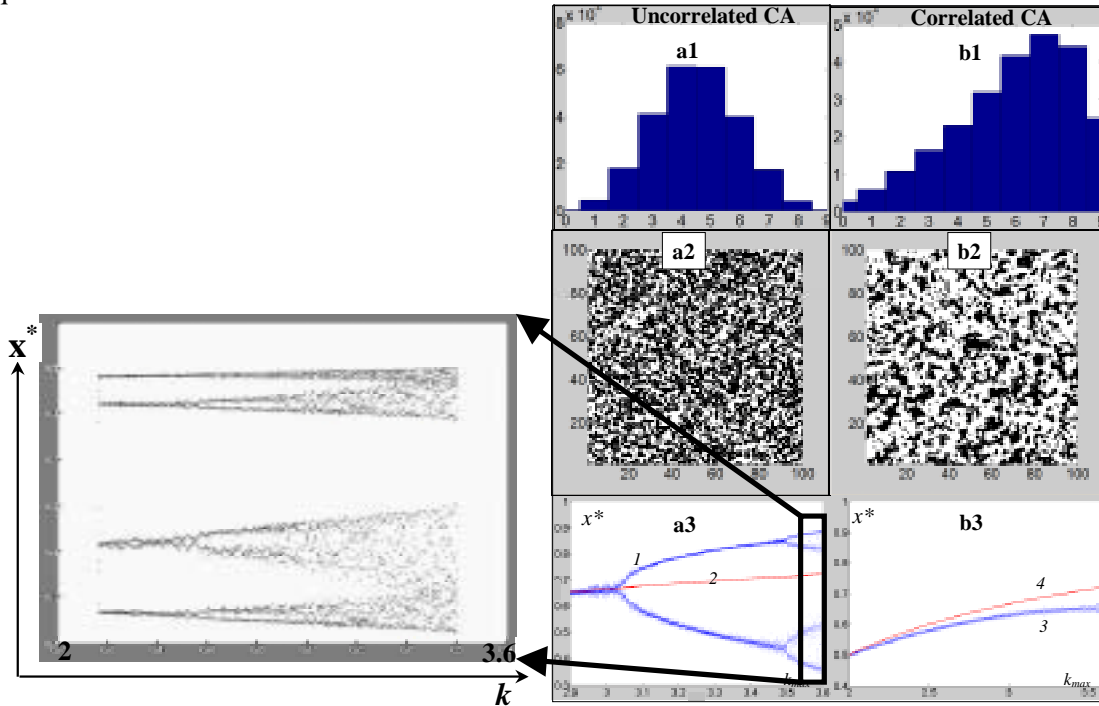
Fig.5 Selected results from two classes of discrete cellular automata systems representing "uncorrelated" - the left panel - and "correlated" – the right one - populations. The histograms (a1,b1) represent the probability of finding from 0 to 9 populated nodes in the Moore neighborhood. The snapshots of contours (a2,b2) on the CA lattice shows the location of populated and unpopulated CA nodes. The white spots mark populated nodes. The average population densities (a3,b3) as the function of k (1,3) are confronted with the function $f(k)=1-1/k$.

In the left panel of Fig.5 we display:

1. the histogram of the number of populated nodes in $\Omega(l,m)\cup\{l,m\}$(a1),
2. contour map (a2) of the CA lattice before random scatter procedure; the white spots stand for populated area ($M=100$),
3. the total population density x as a function of k (a3),

obtained for the "uncorrelated" CA system with totalistic rule **R2** defined by Eg.13. The histogram from Fig.5a1 reproduces well the binomial distribution of neighbors. As shown in Fig.5a2, the CA lattice is populated in a very chaotic way. The logistic map is confronted with the

function $f(k) = \left(1 - \dfrac{1}{k}\right)$. As shown in Fig.5a3, the CA system with microscopic rule **R2**

reconstructs well the part of the logistic map for $k \leq 3.6$ in the macro-scale. The imperfections and noise seen in Fig.5 are the result of the limited accuracy dictated by the size of CA lattice (to obtain Fig.5a3 we used 500x500 lattice) and approximate procedure used for reconstruction of the logistic map.

As shown in the right panel of Fig.5, by disabling the procedure of random scatter (random walk with $\Delta T = \Delta T_{MAX}$), the rule **R2** alone produces global dynamics of CA system which differs substantially from that predicted by the logistic law. The histogram of nearest neighbors (b1) is different than the binomial distribution (a1), larger spatial structures emerge on the lattice (b2) and the population is stable for all values of k (b3). We can conclude that the spatial structures produced by correlated populations can restrain organisms to encounter each other proportionally to their average density. This way, the spatial patterns can postpone or inhibit completely the chaotic changes in average population density.

To show the influence of population motility on the global system dynamics we enable the random walk rule **R1** with growing ΔT. The value of ΔT is equal to the number of random walk steps allowed before the **R2** evaluation rule. The random walk is realized employing HPP lattice gas described in Chopard and Droz book [10]. This model is discrete equivalent of the classic diffusion-reaction model of ecological import, which represents logistic population evolution with Brownian random dispersal [9]. As shown in Fig.6, for $\Delta T = 10000$, the fluctuations of population density are very similar to that observed for the "uncorrelated" model. Due to the fast diffusion, the discrete systems can develop chaos. This effect can be strengthen additionally by combining diffusion with greater neighborhood $\Omega(l,m)$, i.e., by increasing dispersal and competition radiuses. Then, according to Eq.12, the value of maximum biotic potential k_{max} also increases. As shown in Fig.7b, for $r=R=30$, the parabolic phase diagram is reproduced much better than in Fig.7a ($r=R=1$). It means that due to greater neighborhood, the entire CA system can reconstruct better chaotic modes of the logistic map. We showed that the population becomes "logistic" in the limit of infinite motility (ΔT) and the size of neighborhood (N_N). Do we get the same effect by increasing only the local neighborhood $\Omega(l,m)$?
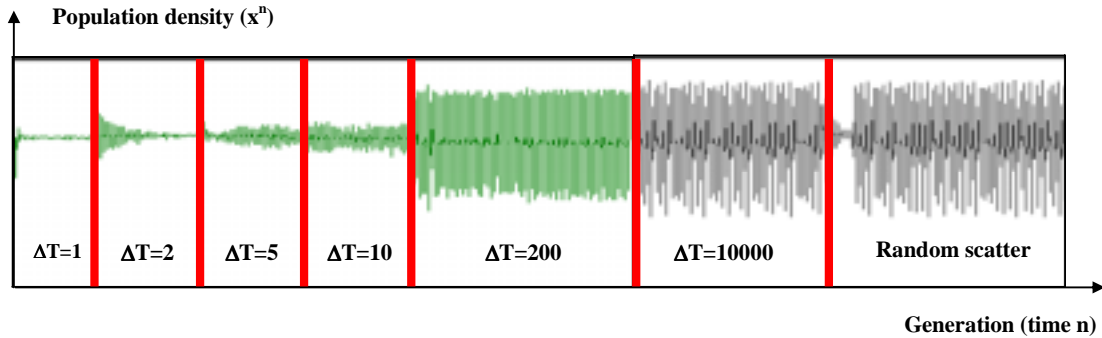
Fig6. The fragments of time series x^n for various population motilities.

As shown in Fig.8, by assuming greater neighborhood for "correlated" CA system we obtain self-similar patterns, which zoom in with increasing $r=R$. These patterns are very unstable due to strong selection pressure caused by competition. The competition destroys dense clusters of the radius equal or greater than $r=R$ allowing for creation of thin "borders" between less populated areas. Because the "borders" vanish very fast due to the strong competition, and compact clusters emerge where the local population density $x \approx 1/2$, the spatial dynamics become oscillating and unpredictable. Despite this intricate dynamics even for relatively large $r=R$ only feeble time

fluctuations of the average population density can be observed. As shown in Fig.9, the signs of chaos can be recorded for the neighborhood diameters $r=R$ comparable to M - the size of the CA lattice. Only then the fast oscillations of large spatial patterns cannot be compensated by reverse oscillation elsewhere on the lattice.
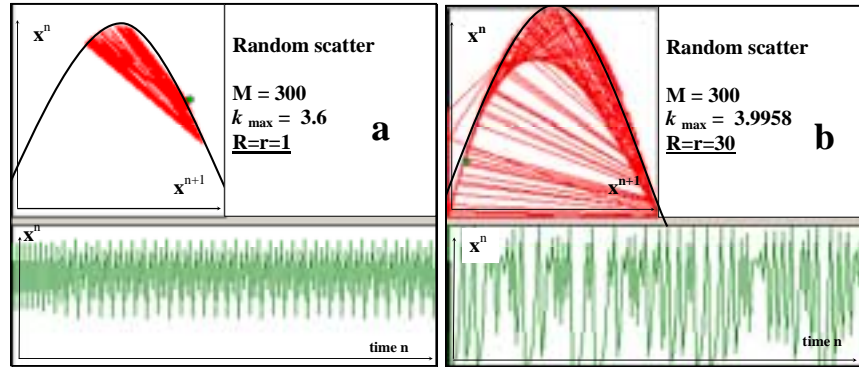
Fig.7 The phase diagrams for the "uncorrelated" CA system for different dispersal and competition radiuses. a) For the Moore neighborhood ($R=r=1$), the system just started to be chaotic. b) The chaos develops for increasing number of neighbors (see Eqs.12).
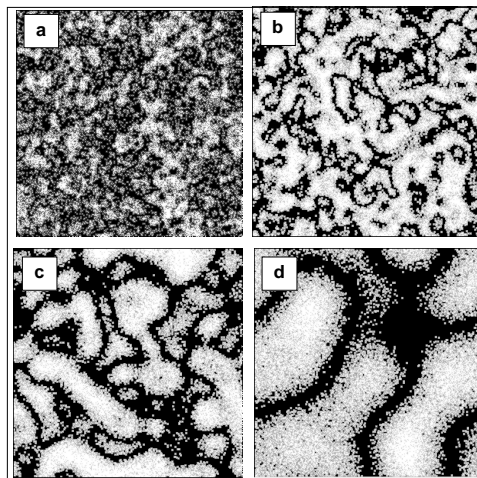
Fig.8 The self-similar patterns produced on the CA 300x300 lattice for the "correlated" population model assuming $r=R=$ a) 3 b) 10 c) 20 d) 50. The black dots stand for populated nodes.
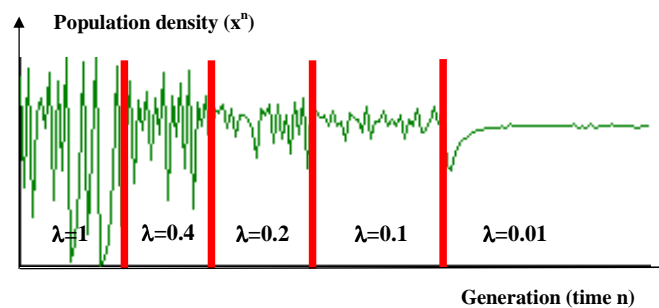
Fig.9 The fragments of plots showing the changes of population density x in time for the motionless "correlated" CA system for various aspect ratios $\lambda=(2 \cdot R+1)/M$.

Let us wonder now what will happen when radiuses of dispersal R and competition r are different. As shown in [4,9], such the break in symmetry between dispersal and competition is very common in realistic populations. Different r and R radiuses may cause the values of a (see Eq.13) be greater than one. To eliminate this effect we modified Eq.13 assuming that a, is a sort of fitness factor of individual. The probability that a certain node will be populated in the following round $(n+1)$ is equal to:

$$f(a) = \begin{cases} a & a < 1 \\ 1 & a \geq 1 \end{cases} \tag{14}$$

By increasing $r/R >> 1$ ratio, i.e., the competition (r) is greater then dispersal (R), the stabilizing influence of competition allows for existence of stable clusters with radius less than r and greater than R. It is easy to deduce that the optimal forms of clusters are strips and clumps. As shown in Fig.10, the simulation results confirm this conjecture.

The similar patterns were observed in [4] for PDE predator-prey model with explicit diffusion term. They are generated purely by the dynamics of the interactions between the predators and pray assuming that diffusion rate of predator is sufficiently greater than the diffusion of the pray. Then the stabilizing influence of the predator may be dissipated by diffusion, yielding regular peaks and streaks of prey and predator densities. The reasons of creation of the same patterns by our model are similar. This time, however, instead of diffusion the large competition radius decreases the competition pressure allowing for increase of the local density of population. Unlike the situation from Fig.5b3, the average density of population as a function of k, $x^*(k)$, matches well with function $f(k)=1-1/k$. For small values of k (small population density) strips are getting unstable and they collapse into clumps. However, the number of rows remains the same for a given system size (M) and for the value of competition radius r (assuming dispersal $R=1$). It is easy to asses that the estimated number of rows is then:

$$l \approx \text{int}\left(\frac{2}{3}\frac{M}{r}\right) + 1 \tag{15}$$

This stable dynamics and patterns become more and more chaotic with decreasing r/R ratio and with increasing r. When the ratio approaches 2, the spatial distribution becomes completely chaotic and the whole system behaves in the logistic way.
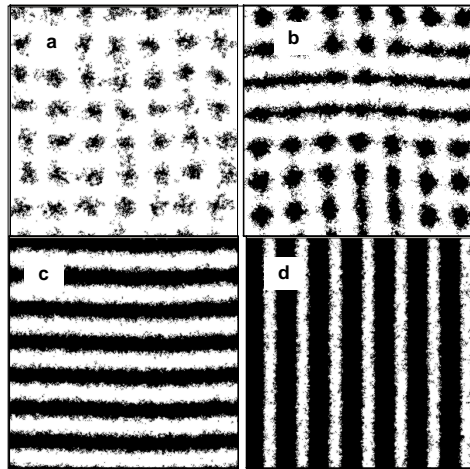
Fig.10 The regular and stable patterns created by the discrete "correlated" CA system for, $M=200$, $R=1$ and $r=30$: a) $k=1.15$, $t=3000$, $x^*=0.13$; b) $k=1.4$, $t=600$, $x^*=0.31$; c) $k=2$, $t=600$, $x^*=0.51$; d) $k=4$, $t=600$, $x^*=0.73$, where t is the number of time-steps and x^* is the average population density. From Eq.15 the number of rows is $l=7$.

The reverse situation, that is, when dispersal (R) is greater then competition (r) and $R/r>1,$ is less realistic. On the one hand the tight competition destroy dense cluster. On the other, it creates them in the empty areas, which are sufficiently close to the clusters. The large dispersal stabilizes average population density. This alternate interactions cause that for $k>2$ instead of stable *streaks_and_clumps* patterns, only oscillating streaks are observed. Otherwise, for $k<2$, the population distribution on the lattice becomes chaotic. In the both cases the average density $x*$ is constant in time if $R>>r$. As shown in Fig.8, if $R/r\rightarrow2$ and R is comparable to the lattice size, the period doubling bifurcation is observed and x* starts to oscillate. We do not observe, however, any bifurcation cascades and any signs of chaos characteristic for logistic dynamics. By assuming different shapes of the local neighborhood inspected (e.g. more realistic circular shape instead of rectangular neighborhood considered here), heterogeneous environment and high diversification of the population, more sophisticated spatial patterns can be created (see e.g. [6,7,8,14,19,20,25]).
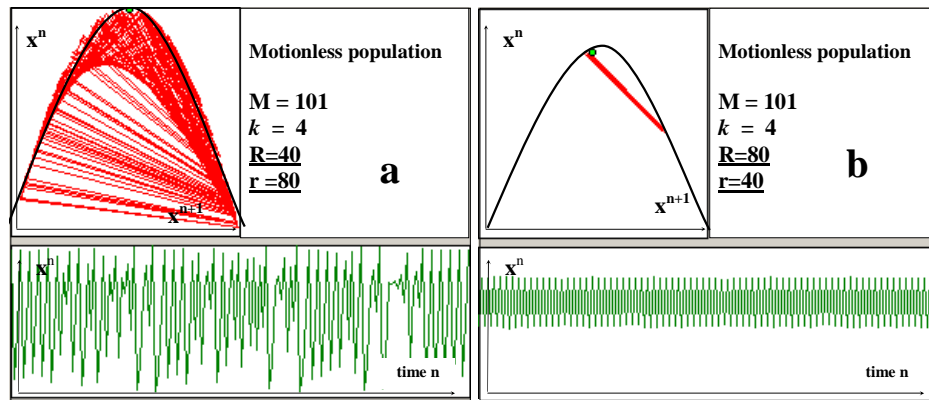
Fig.11 The phase diagrams and the average population density as the function of time for the discrete "correlated" population with two "reverse" dispersal/competition (r/R) ratios.

4   Concluding remarks

There are many reasons why the ecological models, like the logistic equation, fail to give an adequate description of the population growth [4]. However, there are two factors of fundamental importance - neglected in simplistic models - which influence the population dynamics the most:
1.   the space in which the colony evolves,
2.   the variety of ways the individuals interact with their neighbors.

The microscopic interactions are defined, as a combination of an explicit mathematical formula and the size&shape of the neighborhood influenced by a single individual. In more advanced models the interactions between the colony and environment, the heterogeneity of the two and external agents must be considered. But here, we do not discuss these factors assuming that they are of secondary character.

Both the space and interaction rules are tightly coupled. Therefore, the final spatio-temporal dynamics and emergent phenomena are just a consequence of heavy feedback between the spatially extended environment and the ways the individuals interact. So, there is no curiosity in that the logistic equation can fail in describing time evolution of many organisms. More intriguing is the question why in many cases the logistic pathway matches the realistic patterns of population growth. In this paper we tried to answer when such the fundamental factors like space and interactions cancel out and the spatially extended system behaves according to the scenario

described by the logistic model. We studied these problems modeling the spatially extended population on the CA lattice.

We considered first the CA lattice of tightly coupled logistic systems represented by cellular automata with continuous states. This system mimics a large population of many subpopulations interacting with their local neighbors according to the semi-logistic rule (Eq.5). We showed that the global behavior of this system (i.e. the time evolution of the average population density) match perfectly the logistic law for the value of biotic potential $k<k_\infty$ The population density becomes uniform in every time moment on the entire lattice until $k<k_\infty$. For $k>k_\infty$ when the chaotic dynamics is expected, the system stabilizes. However, instead of uniform (but oscillating in time) distribution, the population density diversifies progressively with increasing k. The intricate evolution of spatial patterns, represented by irregular clusters, can be observed. We can conclude that the global chaotic temporal behavior is transferred spontaneously into spatial chaos. This transition can represent a kind of self-preservation mechanisms. The system consisting of many subpopulations interacting according to the rule given by Eq.5 cannot be destabilized (be chaotic) by increasing the value of biotic potential, i.e., by increasing the reproduction potential of population.

Going downscale, we considered a single subpopulation from the previous continuous model as a separate spatially extended system modeled on the cellular automata lattice. This time however, it represents colony of discrete entities. We showed that "uncorrelated", randomly scattered populations evolving on 2-D CA lattice can mimic the same pathway to chaos as the logistic model, i.e., the evolution from stable colonies through bifurcation cascades to chaos. This global logistic map can be obtained for selected type of microscopic CA rules. We showed that the fully developed chaotic behavior ($k_{max}=4$) occurs only for infinitely large dispersal and competition radiuses. For the Moore neighborhood the maximal biotic potential is $k_{max}=3.6$, a little bit greater than the accumulation point $k_\infty \approx 3.5699$, i.e., the moment of onset of chaos. For von Neumann neighborhood ($k_{max}=3,33(3)$) only the first bifurcation can occur. Due to random scatter, the population distribution is approximately uniform and only small, random patterns develop.

The same rules were applied for motionless (without scatter) CA system with limited neighborhood capacity. However it produces only stable populations with average population densities remaining constant in time. Simplicity in temporal dynamics is accompanied by the complex spatial dynamics with dynamically changing patterns. Contrary to very similar, in spirit, continuous CA, the time evolution of average population density is different from the logistic map for every value of k. We showed that

1. by allowing for random walk of individuals between evaluation rounds,
2. by increasing dispersal and competition, i.e., the size of the neighborhood,
3. by assuming a certain ratio (≈ 2) between competition and dispersal radiuses,

the stable system can be transformed to chaotic or partly chaotic and be more similar to the logistic map. The steady-state fragment of the logistic map ($k<3$) can be also reconstructed by the systems producing stable patterns: clumps and strips. We show that such the patterns can be obtained assuming the ratio of competition and dispersal radiuses large enough.

The role of disorder and spatial patterns in control of population dynamics is well known [1,26,27]. Our results show that the spatially extended systems with population uniformly distributed in space, reproduce better the fragment of the logistic map representing bifurcation cascades and chaos. The populations forming dynamically changing spatial clusters and stable patterns behave in a different way than the logistic model and reproduce at least steady-state fragment of the logistic map.

The dynamics described by the logistic map is very diverse and extends from stable behavior, bifurcation cascades up to the chaotic modes. The knowledge that a certain population matches logistic pathway to chaos may have very important consequences for its future. When the

average population density is oscillating or chaotic, the colony becomes vulnerable on external threats, e.g., pestilences [13]. Additional degrees of freedom defined by space and microscopic interactions between individuals allows for creating "self-preservation instinct" and more flexible reaction of the population on the external danger. Scrutinizing the ways the adverse effects of chaotic evolution can be eliminated, is fundamental to protect the colony from extinction. Conversely, the knowledge about the ways the chaos develops can allow for eliminating the structured populations, which are very difficult to destroy, and which can be very dangerous such as the bacterial biofilms [28].

References

1. Kaneko K., Tsuda, I., (2001). *Complex Systems: Chaos and beyond*, Springer Verlag, 273 p.
2. Kendall, B.E., (1998). Spatial Structure, Environmental Heterogeneity, and Population Dynamics: Analysis of the Coupled Logistic Map, *Theor. Popul. Biol.,* 54, 11-37.
3. Lloyd, A.L., (1995). The Coupled Logistic Map: A Simple Model For The Effects of Spatial Heterogeneity on Population Dynamics, *J. Theor. Biol.,* 173, 217-30
4. Law, R., Murrell, D.J., Dieckmann, U., (2003). Population Growth in Space and Time. Spatial Logistic Equation, *Ecology,* 84 (1), 252-262.
5. Bejan A., (2000). Shape and Structure, from Engineering to Nature, Cambridge University Press, p 324.
6. Ben-Jacob, E., http://star.tau.ac.il/~eshel/gallery.html
7. Ben-Jacob E, Cohen I. and Levine H. (2000) Cooperative self-organization of microorganisms, *Adv. Phys.* 49(4):395-554
8. Cohen I. Golding I. Kozlovsky Y. and Ben-Jacob E. (1999) Continuous and discrete models of cooperation in complex bacterial colonies. *Fractals* **7**:235-247
9. Holmes, E.E., Lewis, M.,A., Banks, J.E., Veit, R.R., (1994). Partial differential equations in ecology: Spatial interactions and population dynamics, *Ecology,* 75(1), 17-29.
10. Chopard, B., Droz, M., (1998). Cellular Automata Modeling of Physical Systems (Cambridge University Press,Cambridge, England).
11. Wolfram, S., (2002) A New Kind of Science, Wolfram Media Incorporated, p 1263.
12. Yang Xin-She, Young, Y. (2006). Cellular Automata, PDEs, and Pattern Formation, in Handbook of Bioinspired Algorithms and Applications, eds. Olariu S., Zomaya A.Y., Chapman & Hall/CRC, Boca Raton, London, New York, 273-284.
13. Dzwinel W, Yuen DA, (2005). Aging in Hostile Environments Modeled by Cellular Automata with Genetic Dynamics*, Int. J. Modern Phys. C*, 16, 3, 357-377
14. Krawczyk K, Dzwinel W, Yuen DA, (2003). Nonlinear Development of Bacterial Colony Modeled with Cellular Automata and Agent Objects, *Int. J. Modern Phys. C*, 14,10, 1385-1404
15. Grimm, V., Railsback, S.,F., (2005) *Individual-Based Modelling and Ecology*, Princeton University Press: Princeton, NJ, 480 pp
16. Murrell, D.,J., Dieckmann, U., Law, R., (2004). On moment closures for population dynamics in continuous space, *Journal of Theoretical Biology*, 229, 421–432
17. Ellner, S., P., (2001) Pair Approximation for Lattice Models with Multiple Interaction Scales, *J. theor. Biol*. 210, 435-447

18. Schuster A.G., (1993). Deterministic chaos. Wydawnictwo Naukowe PWN (Polish edition) p.274
19. Abbey, D., http://www.ganymeta.org/~darren/patterns.php
20. Franks, P.J.S., (1997) Spatial patterns in dense algal blooms, *Limnol. Oceanogr.* 42(5/2), 2997-1305
21. Topa P., Dzwinel W., Yuen, D.A., (2006). A multiscale cellular automata model for simulating complex transportation systems, *Int. J. Modern Phys. C*, 17/10, 1437-60
22. Phatak, S.C., Rao, S.,S., (1995). Logistic Map: A possible random-number generator, *Phys. Rev. E.,* 51(4), 3670-78.
23. Amritkar, R.,E., Gade, P.,M., (1993). Wavelength Doubling Bifurcations in Coupled Map Lattices, *Phys. Rev. Lett*. 70(22):3408-11
24. Thompson, H., R., (1956). Distribution of distance to *N*-th neighbour in a population of randomly distributed individuals, *Ecology,* 37/2, 391-394,
25. Lacasta, A.M., Cantalapiedra, I.R., Auguet, C.E., Penaranda, A., and Ramı́rez-Piscina L., (1999). Modeling of spatiotemporal patterns in bacterial colonies, *Phys. Rev. E.,* 59(6), 7036-41
26. Kaneko, K., (1989) Pattern dynamics in spatio temporal chaos, *Physica D* 34 (1989) 1-41
27. Braiman Y., Lindner, J., F., Ditto, W., L., (1995), Taming spatio-temporal patterns with disorder, *Nature,* 378, 465-7
28. Pizarro, G., Griffeath, D., Noguera, D., R., (2001). Quantitative Cellular Automaton Model for Biofilms, *Journal of Environmental Engineering*, 127/9, 782-789.